



## Article

# Pyrolysis of RDF and Catalytic Decomposition of the Produced Tar in a Char Bed Secondary Reactor as an Efficient Source of Syngas

Bogusław Kusz<sup>1</sup>, Dariusz Kardaś<sup>2,\*</sup> , Łukasz Heda<sup>1,2</sup> and Bartosz Trawiński<sup>1</sup> 

<sup>1</sup> Faculty of Applied Physics and Mathematics, Institute of Nanotechnology and Materials Engineering, Gdańsk University of Technology, Narutowicza 11/12, 80-233 Gdansk, Poland; bogkusz@pg.edu.pl (B.K.); lukasz.heda@imp.gda.pl (Ł.H.); bartosz.trawinski@pg.edu.pl (B.T.)

<sup>2</sup> Institute of Fluid Flow Machinery, Polish Academy of Sciences, Fiszerza 14, 80-231 Gdansk, Poland

\* Correspondence: dk@imp.gda.pl

**Abstract:** One of the technical limitations of refuse-derived fuel (RDF) pyrolysis is the high content of tar in its gas products. In order to resolve this problem, a two-stage RDF pyrolysis with a catalyst based on char from RDF pyrolysis is proposed. This paper presents the results of municipal waste pyrolysis beginning in an oven heated to 480 °C and ending with catalytic tar cracking carried out in the temperature range from 800 to 1000 °C. Thermal and catalytic pyrolysis with a char catalyst containing a minimum of 6% Fe resulted in increases in the CO and H<sub>2</sub> contents in gas products and decreases in CO<sub>2</sub> and CH<sub>4</sub>. At 1000 °C, the mass ratio of gaseous products to liquids was greater than 6. The residence time of the gases in the catalytic zone was about 3–5 s. The reactor was a good source of hydrogen and carbon monoxide.

**Keywords:** pyrolysis; catalyst; cracking; municipal solid waste; residence time



**Citation:** Kusz, B.; Kardaś, D.; Heda, Ł.; Trawiński, B. Pyrolysis of RDF and Catalytic Decomposition of the Produced Tar in a Char Bed Secondary Reactor as an Efficient Source of Syngas. *Processes* **2022**, *10*, 90. <https://doi.org/10.3390/pr10010090>

Academic Editors: Carmen Branca and Antonio Galgano

Received: 19 October 2021

Accepted: 17 December 2021

Published: 2 January 2022

**Publisher's Note:** MDPI stays neutral with regard to jurisdictional claims in published maps and institutional affiliations.



**Copyright:** © 2022 by the authors. Licensee MDPI, Basel, Switzerland. This article is an open access article distributed under the terms and conditions of the Creative Commons Attribution (CC BY) license (<https://creativecommons.org/licenses/by/4.0/>).

## 1. Introduction

In the European Union (EU), 250 million tons of municipal waste is generated annually, which means that each inhabitant produces an average of 488 kg of waste per year [1]. There are big differences in the production of waste in the different countries of the EU. The largest amount per capita per year is produced in Denmark and is 766 kg, while the least is produced in Romania and is 266 kg. Waste production and use in the countries of the old EU (EU15: Austria, Belgium, Denmark, Finland, France, Greece, Spain, the Netherlands, Ireland, Luxembourg, Germany, Portugal, Sweden, Great Britain, and Italy) differ from those in the new member countries of the EU (EU13: Bulgaria, Czech Republic, Estonia, Croatia, Cyprus, Latvia, Lithuania, Hungary, Malta, Poland, Romania, Slovakia, and Slovenia). The division into the countries of the old and the new EU is clearly seen in the comparison of methods of using municipal waste, as shown in Table 1. In the EU15 countries, 208 million tons of municipal waste is processed every year, which represents an average of 511 kg of waste per inhabitant, while the residents of the EU13 countries produce 34.9 million tons, which represents 335 kg per inhabitant. The differences between the countries of the old EU15 and the new EU13 include not just the amount of waste produced. In the EU15 countries, 31% of the waste is recycled, whereas in the EU13, the corresponding figure is 24%. Moreover, in the EU15 countries, 31% of the waste is used in waste-to-energy processes, while in the EU13, only half as much, or 15%, is processed in this way. These proportions are different in the case of landfilling: in the EU13, as much as 53% of the waste is treated in this way, while in the EU15, only 18% goes to landfill. The rest is composted.

**Table 1.** Statistics for treated municipal waste in the EU15, EU13, and Poland (PL) [1].

	Treated MSW, Kt			Treated MSW Per Capita, kg			Percentage of Treatment, %		
	EU15	EU13	PL	EU15	EU13	PL	EU15	EU13	PL
Recycling	65,511	8300	3199	161	80	84	31	24	27
Incineration	64,705	5280	2922	159	51	77	31	15	24
Composting	38,702	2774	848	95	27	22	19	8	7
Landfill	39,187	18,546	5000	96	178	132	19	53	42
Sum	208,105	34,900	11,969	511	335	315	100	100	100

Poland has 38 million inhabitants and is the largest of the EU13 countries. In 2017, its production and processing of municipal waste amounted to almost 12 million ton (Table 1). Calculated per capita, this represents 315 kg per person, which is one of the lowest amounts not only in the entire EU but also among the EU13 countries. In Poland, as well as in the EU13 countries, the largest part of the waste is stored (42%), while 24% is subject to heat treatment. Comparing the EU15 and EU13 countries and Poland, the smallest differences can be seen in the recycling category. The energetic use of waste in Poland is relatively large (24%) due to the significant involvement of the cement industry, which uses part of the waste as fuel in furnaces. In addition to cement plants, municipal waste is incinerated in eight incinerators operating near large cities, in which 849 ton of waste was thermally processed in 2017. In principle, it is not possible to increase the amount of waste used in the existing municipal and cement installations, and, therefore, new waste incineration plants are needed. Thirty-five waste thermal installations with capacities from 7000 to over 100,000 ton/year are being planned by the provincial waste management throughout Poland. Most of the planned incineration plants would have a relatively low capacity, from 7000 to 30,000 ton/year, but only large plants with capacities of 100,000 and 160,000 ton/year are being constructed in Rzeszów and Gdańsk, respectively [2]. This is due to economic reasons: only large, rich cities are able to raise funds for the construction of expensive investments, such as the EUR 120 million raised for the construction of a waste incineration plant in Gdańsk. The vast majority of waste incineration plants are based on the technology of boilers with a movable grate, because as many as 87% of all incineration plants in Europe, and 80% in the world, are equipped with movable grates [3,4]. Combustion installations convert the chemical energy of the waste into thermal energy, from which electricity is produced. The way it is used depends on the technology and the economy, but most often thermal energy is used to produce electricity and municipal heat. Boilers and steam turbines with operating parameters from 180 °C and 10 bar to 400 °C and 40 bar are usually used. The use of steam turbines is expensive and raises the costs of waste-to-energy (WTE) systems, although this is a proven solution.

The problem of waste management coincides with the development of the hydrogen-based economy. A hydrogen economy, developing as a result of shifting away from fossil fuel, brings a need for hydrogen obtained using renewable energy and other environmentally friendly resources [5]. Pyrolysis and gasification of organic matter can be a way of obtaining hydrogen. However, some issues need to be overcome, for example, increasing the content of hydrogen in the obtained gas mixture [6,7].

In the case of relatively small WTE systems, an alternative to boilers and steam turbines could be internal combustion engines with electric power generators, which are definitely cheaper in terms of generated power. In such a case, the entire installation consists of a gasification reactor, gas purification and valorization system, an internal combustion engine, and a power generator. There have been many such installations, for example, the Thermoselect installation in Chiba (Japan) [8], which processes 15 tons of waste. A pilot project of an installation for the gasification of municipal waste with a capacity of 100 kg/h was created in Nowy Dwór (Poland) [9] based on a fixed-bed reactor equipped with a



syngas combustion chamber. In general, gasification technologies for municipal waste have not reached a level that would allow their commercialization.

Another method of producing combustible gases from waste is the pyrolysis process, whose course is regulated by heat supplied from the outside, which improves control. There are several types of pyrolysis methods, among which the following can be distinguished: the fixed-bed reactor, rotary kiln, fluidized-bed, and tubular reactors [10–12]. The use of pyrolysis gases in internal combustion engines is associated with the problem of tar, which accumulates on the surfaces of the transport pipelines and engine components and locks the engine rapidly. The removal or drastic reduction of the tar in the gas would facilitate the development of municipal waste pyrolysis technology.

In general, pyrolysis of solid fuels and waste produces char, noncondensing gases, and oils and liquids. A review of liquid/tar reduction methods in wood gasification products presented by Devi et al. [13] divided cleaning technologies into primary methods (inside the reactor) and secondary methods after gasification. They pointed out the importance of the installation operating parameters for the tar content and discussed the applications of additives such as dolomite, olivine, and coal inside the reactor. As a good catalyst for tar decomposition processes, Ni was proposed, although it is an expensive metal.

The influence of pyrolysis temperature and catalysts has been the subject of many studies. Table 2 presents the results of studies by selected researchers [14–19], who pyrolyzed biomass and various wastes and measured the share of gaseous, liquid, and solid products.

**Table 2.** Parameters of municipal solid waste (MSW), biomass pyrolysis (BM), plastic waste (PW), residue-derived fuel (RDF), plastic and paper waste, and product distribution.

Fuel	Temperature, °C	Catalyst	Gas, %	Liquid, %	Solid, %
		Kardaś et al. [14]			
MSW	500		14	43	43
MSW	900		48	30	22
		Al-Rahbi et al. [15]			
BM	600		22.4	49	24
BM	800		46.6	28.5	23
BM	600	Tyre char	31	34	24.5
BM	800	Tyre char	57.5	8.5	23.5
BM	600	RDF char	33	43.5	24
BM	800	RDF char	59.5	17	23.5
		Lu et al. [16]			
PW	700	Biochar	56.1	20.2	20
PW	900	Biochar	61.6	12.3	20.1
		Efika et al. [17]			
RDF	700		43.6	29	22.4
RDF	900		52.3	23	21
		Ates et al. [18]			
MSW	500		13	32	55
MSW	600		22	58	20
		Fekhar et al. [19]			
PPW	550		24	48	28
PPW	550	Ni/zeolite	38	35	27

The above shows that the method of reducing the amount of tar is temperature. The pyrolysis temperature is related to the maximum temperature that is reached for the fuel. For typical pyrolysis of solid fuel, the temperature of the fuel and gas products increases from the initial to the maximum temperature. The products of such a process conducted at low temperature contain chemical compounds with high molecular weight that cannot be further decomposed. Additional heating of the primary pyrolysis products at higher temperature results in all of the gaseous pyrolysis products reaching a similar high temperature. Consequently, changes in the amount of gas and liquid products are



observed. It is a fact confirmed in practice that an increase in temperature causes a decrease in the amount of liquid products and an increase in the amount of gaseous products.

Song et al. [20] investigated the problem of MSW pyrolysis with the addition of iron ore. In a TGA analysis, they showed that the addition of iron ore and iron oxide results in a significant reduction in the average activation energy of the MSW. The use of iron ore and iron oxides is cheaper than the use of nickel.

A char-supported Ni-Fe catalyst [21] was found to gasify tars with over 90% efficiency. Iron ore was also found to enhance the gasification of tar [22]. This process occurs above 650 °C. At lower temperatures, carbon deposits are produced.

In a review article on the thermal and catalytic pyrolysis of plastic waste [23], a wide range of problems related to the pyrolysis of plastic waste were addressed, including an analysis of the impact of the duration of the process on the decomposition of the catalytic product, the temperature, the pressure, and catalysts. Gas residence times below two seconds at 650–800 °C cause a significant increase in gas content, by several percentage points, in pyrolysis products. The catalytic pyrolysis has some advantages over the thermal process as it improves performance by reducing the residence time in the process and affects the product selectivity. In addition, catalytic cracking through the use of zeolites produces a fuel that is suitable for internal combustion engines.

Al-Asadi and Miskolczi [24] conducted tests on the pyrolysis of a real mixture of plastic waste (mainly LDPE, HDPE, PP, and PET) at 700 °C. The pyrolysis was carried out using catalysts in the form of zeolite containing nickel, calcium, cerium, lanthanum, magnesia, or manganese. The influence of the Me/Ni catalyst ratios on the pyrolysis products was investigated. The ratio of the two metals did not significantly affect the yield of volatile substances. In general, the inclusion of a second metal in the catalyst structure can support a lower distribution of the main polymer chains.

The practical application of MSW (including RDF) pyrolysis in small, local landfills requires a high level of tar cracking, low costs, and simple technology. There is a need for a simple and cheap method of tar decomposition to obtain the maximum amount of useful gas with high hydrogen content. The present paper aims to evaluate the degree of reduction and purification gas formed as a result of pyrolysis of the RDF permeating as a result of overpressure through the RDF char heated to temperatures from 800 to 1000 °C.

The research was carried out with a reactor operating without nitrogen as a carrier gas, without steam supporting the formation of H<sub>2</sub>, and with the char obtained from RDF used for reducing and purifying the gas obtained from RDF pyrolysis. The influence of the addition of a nanostructured iron catalyst to the char was investigated.

## 2. Materials and Methods

### 2.1. Feedstock

Municipal waste from the landfill in Olsztyn was used for this research. It contained mainly plastics, clothing, paper, and metals. The waste was pelleted to a diameter of 6 mm, length of 5–25 mm, and bulk density of 0.51 kg/dm<sup>3</sup> and was used in the experiments in this form. This class 2 RDF comes from a mechanical waste processing line and meets the requirements of EN-15359: 2012. Technical analysis of the RDF gave 40.8 wt% char and 59.2 wt% volatile. TGA was used to determine these parameters. The heat of combustion (HHV) of the municipal waste was 22.1 MJ/kg, as determined using an Ekotechlab Series 500 calorimeter. The RDF was used for the tests after two hours of drying with a moisture content less than 1%.

Elemental analysis was performed using a Thermo Scientific Flash 2000 CHSN/O Analyzer and gave a result of 46.5 wt% carbon, 6.6 wt% hydrogen, and 36.4 wt% oxygen (by difference) (Table 3). Using an EDAX Genesis APEX 2 and ApolloX SDD, the share of the remaining elements was determined and mainly comprised 1.2 wt% Si, 3.0 wt% Ca, and 1.0 wt% Fe.

**Table 3.** Elemental analysis (wt%) of RDF and catalysts from RDF.

	RDF	ChFe11	Catalyst ChFe6	ChFe1
C	46.5	54.0	56.0	80.0
H	6.6			
O	36.4			
Na	0.9	1.5	1.3	0.7
Mg	0.2	1.1	1.1	0.5
Al	0.9	2.8	3.5	2.0
Si	1.2	10.0	10.4	9.8
P	0.2	3.3	3.5	0.2
S	0.6	0.9	1.1	0.5
Cl	0.6	2.2	2.3	0.9
K	0.2	1.2	1.2	0.6
Ca	3.0	10.6	13.0	2.3
Ti	0.2	0.9	1.3	0.9
Fe	1.0	10.4	5.5	1.6

## 2.2. Test-Bench

The test-bench for testing the catalytic waste pyrolysis consisted of a gas-tight chamber filled with RDF pellets in one place and char in another, two heating furnaces, a scrubber system, and a gas-thigh bag collecting the produced gas (Figure 1a). The chamber itself was made of horizontally placed quartz glass with a diameter of 30 mm and a length of 1 m. In the first furnace, the RDF samples were heated gradually to 480 °C and the rate of increase of the furnace temperature was 3 °C/min. Gas samples were taken in sample bags when the temperature of the RDF sample was equal to 350, 410, and 480 °C. The second furnace heated the char to a constant temperature of 800, 900, or 1000 °C in different experiments. The quartz tube was closed with vacuum-tight flanges, with a gas outlet pipe passing through one of them (Figure 1b). The RDF charge weighed approximately 32 g each time; it took up a length of 15 cm and was held by ceramic wool spacers of 2 cm in length each. The catalyst layer of char heated by the second furnace was 20 cm long and was also limited by 2 cm of mineral wool. The thermocouples T1 and T2 measured the temperature inside the RDF and in the catalyst char bed. In the experiment, no additional gases were used to lift the pyrolysis products, as was the case in Al-Rahbi et al. [15] and Veses et al. [25]. The flow was caused by higher pressure in the tubular reactor than in the gas bag. In this experiment, the gas that formed inside the chamber as a result of the pyrolysis of RDF had an overpressure of 1500–3000 Pa.

As a result of the heating of the RDF samples, the gaseous pyrolysis products first flowed through a bed of hot carbonizate and then through a system of three scrubbers filled with isopropanol, where the condensation of the tar components (polycyclic aromatic hydrocarbons, PAH) took place. The remainder of the pyrolysis gas products flowed into the Tedlar gas bag.

The gases collected in the bags were analyzed by means of a Thermo Fisher Scientific model Trace 1310 chromatograph equipped with a TCD detector. The results were averaged after each series of measurements. The measurement of the volume obtained after reduction and purification of the pyrolysis gas was carried out using a water tank with a movable top cover, maintaining the gas pressure at atmospheric pressure. In addition, the weight of the RDF was measured before the pyrolysis and the char weight was measured after the pyrolysis.

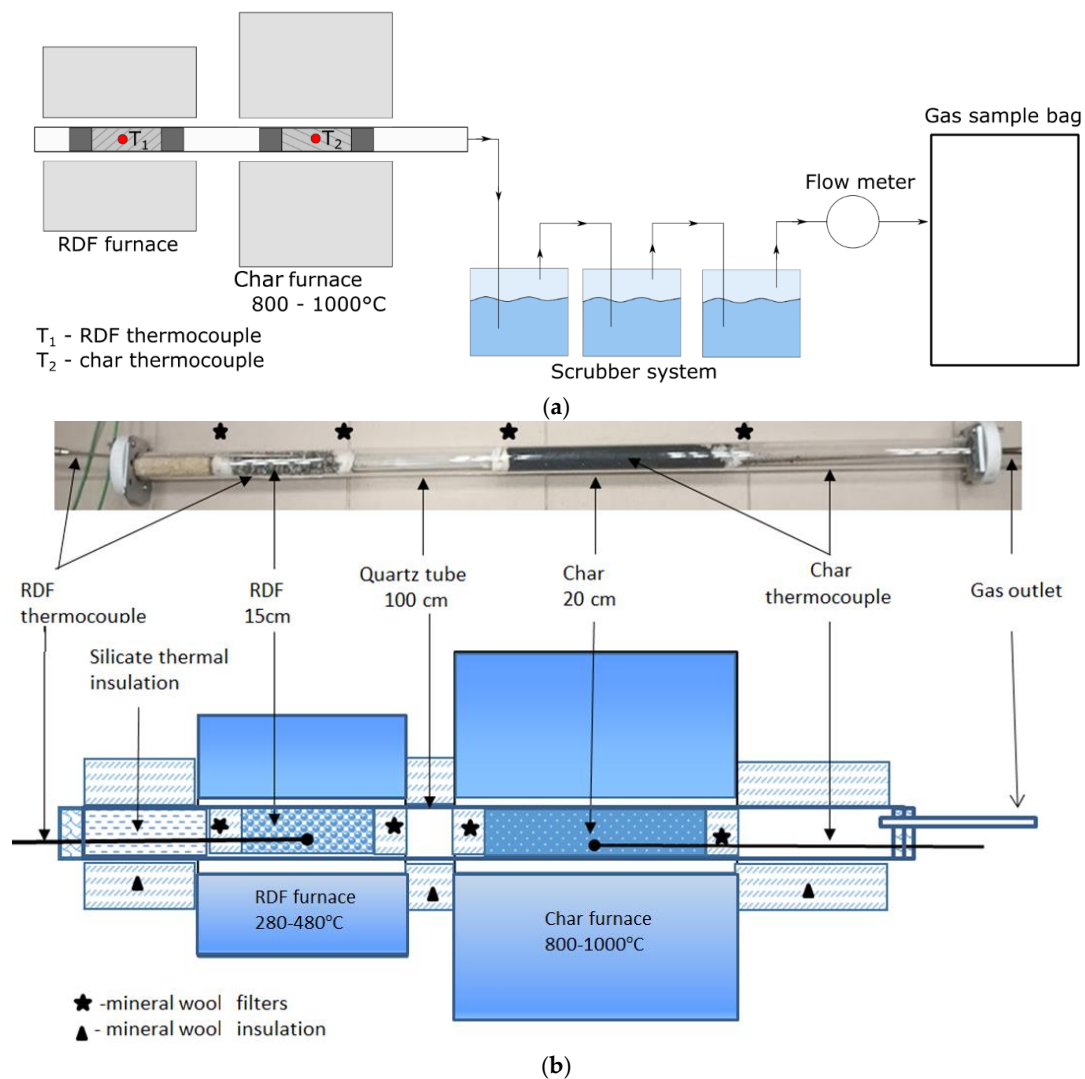


**Figure 1.** Experimental stand: (a) test-bed (schematic diagram); (b) two-furnace RDF pyrolysis setup; top photograph: chamber of the pyrolysis system; bottom schematic diagram: the pyrolysis system.

### 2.3. Catalyst

In the RDF pyrolysis experiment, the pyrolytic gas was cracked in a high-temperature-heated char bed. The tests were carried out at temperatures of the char bed of 800, 900, and 1000 °C. Three types of catalytic char bed were used in the experiments. The first catalyst, designated ChFe6-800, ChFe6-900, and ChFe6-1000, contained about 6 wt% Fe and was obtained after RDF pyrolysis. The second, designated ChFe11-800, ChFe11-900, and ChFe11-1000, was obtained by mixing the char obtained as a result of the pyrolysis of RDF with a fair amount of Fe<sub>2</sub>O<sub>3</sub>. During pre-heating, Fe<sub>2</sub>O<sub>3</sub> was reduced and a layer of catalytic char containing about 11 wt% iron was formed. The third, designated ChFe1-1000, was a char obtained as a result of the pyrolysis of RDF treated with HCl to remove most of the Fe. It should be noticed that HCl also removes most of the other metals. Al-Rahbi and Williams [7] showed that after metal additives are removed, the char has little catalytic activity. The elemental composition of the catalytic char is given in Table 2. The different RDF pyrolysis experiments are hereinafter denoted by the catalyst type and catalyst temperature, for example, ChFe6-900. To obtain reliable results, all eight experiments were performed twice—processes, in which measurements were performed, were predeceased with trial ones, with respective configurations of catalyst and catalyst temperature.

In addition to elemental analysis, an analysis of the crystal structure of the char catalyst samples was investigated by the XRD method using a Bruker D2 Phaser diffractometer

with  $\text{CuK}\alpha$  radiation ( $\lambda = 1.542 \text{ \AA}$ ) at room temperature in a  $2\Theta$  range of  $15\text{--}90^\circ$ . HighScore Plus 3.0.2 software by Malvern Panalytical was used for a phase composition analysis, and the determination of the grain size was performed by the Scherrer method. The diffraction pattern of the ChFe6-1000 sample after the RDF pyrolysis experiment is presented in Figure 2a. A raised background in the range of  $15\text{--}35^\circ$  indicates the presence of an amorphous phase. The multiplicity of the diffraction maxima indicates a multiphase composition.  $\text{SiO}_2$  (Powder Diffraction File 089-1961, hexagonal, and 027-0605, cubic) and  $\text{CaCO}_3$  (083-0577, rhombohedral) were identified as the main phases scattering the X-ray radiation. The iron oxides  $\text{FeO}$  (079-1972) and  $\text{Fe}_2\text{O}_3$  (054-0489) were also identified. Figure 2b shows a close-up of a region with the  $25.5^\circ$   $\text{Fe}_2\text{O}_3$  maximum. The latter is the most significant iron oxide maximum; it does not overlap other peaks and was used for calculation of the grain size, which was estimated to be  $21 \pm 7 \text{ nm}$ . A similar order of magnitude of the iron oxide grain size was also found in other samples. SEM imaging of the ChFe6-1000 catalyst (Figure 2b) revealed the presence of particles containing iron. The size of the visible particles is about 200 nm, different from that resulting from the XRD analysis. The low intensity of the evaluated diffraction maximum may result in inaccurate results. On the other hand, the 20 nm iron oxide particles may be invisible in the SEM images.

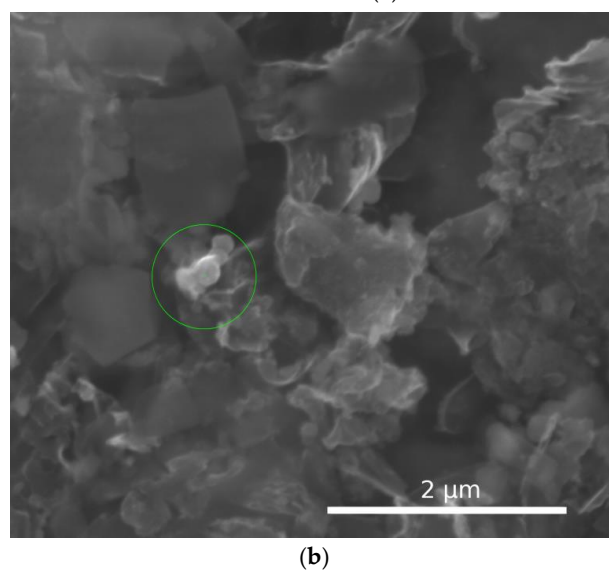
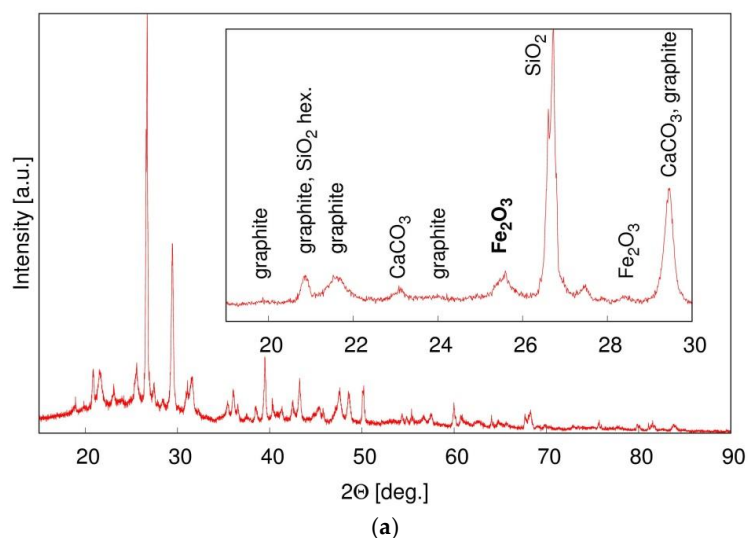


**Figure 2.** (a) Diffraction pattern of ChFe6-1000 sample; inset: close-up of the main maxima; (b) SEM image of the ChFe6-1000 sample with particle identified as iron oxide based on EDX analysis.

### 3. Results

Eight series of tests with RDF pyrolysis and tar cracking were carried out at three different temperatures with various amounts of Fe and are presented in Table 4. Seven series of measurements (ChFe6-800 to ChFe11-1000) were made using a char catalyst with a mass of 90 g each time. The mass fraction of Fe in the catalyst ranged from 1.6 to 10.4%. The tests in the Ch0Fe0-1000 series were conducted without a char catalyst. The heating process of 32 g of RDF was carried out first at a speed of about 10 °C/min from ambient temperature to 300 °C and then at a speed of 3 °C/min to 480 °C. Each experiment lasted about 1.5 h. The average yield of char produced from the pyrolysis of the RDF was approximately 40 wt%. This was constant for all the experiments. The solid particles were also separated in isopropanol and had masses of the order of 30–124 mg, with the largest being obtained in the experiment Ch0Fe0-1000 without additional catalyst (Table 4).

**Table 4.** Characteristics of experiment series: Fe concentration in catalysts and masses of RDF, char, solid, and liquid residues.

Experiment	Fe	RDF	Char Mass, g	Residues	Liquid Mass, mg
	wt%	Mass, g		Solid Mass, mg	
ChFe6-800	5.5	32.2	13.6	55	220
ChFe11-800	10.4	32.3	13.3	50	200
ChFe1-900	1.6	32.3	13.6	30	9.0
ChFe6-900	5.5	32.2	13.5	<0.1	<0.1
ChFe11-900	10.4	32.2	13.4	<0.1	<0.1
ChFe6-1000	5.5	32.1	12.9	35	21.7
ChFe11-1000	10.4	32.3	13.2	40	0.0
Ch0Fe0-1000		32.3	13.3	124	9.8

As part of this research, the quantity and composition of tar were measured by means of a GC-MS GC2010+ GCMS QP2010 Plus. In the measurement series ChFe6-800 at a temperature of 800 °C with catalyst ChFe6, the total amount of products was 220 mg, of which the largest parts were toluene (132 mg), styrene (30.5 mg), and naphthalene (25.3 mg). Temperature increases from 800 °C to 900 and 1000 °C led to a significant decrease in the amount of tar: from an average of 200 mg to 0–20 mg. The results in Table 4 show that a higher content of Fe in the catalyst resulted in a decrease in the amount of tar. At 800 °C with the ChFe6 catalyst, the amount of tar was 220.2 mg, while with the ChFe11 catalyst, this dropped to 200.2 mg. A similar result was obtained in the tests at a cracking temperature of 1000 °C, where 21.7 mg of tar was obtained for 6% Fe, and tar was not measured for 11% Fe.

The gases collected in the Tedlar bags were measured by a TCD gas chromatograph. The composition of the gas obtained at three pyrolysis temperatures, 350, 420, and 480 °C, was investigated. The final results are an average of these gas samples. The gas composition including H<sub>2</sub>, CO, CH<sub>4</sub>, and CO<sub>2</sub> is presented in Figure 3. The remaining O<sub>2</sub> and N<sub>2</sub> accounted for no more than 5 wt%. The results indicate that at a temperature of 800 °C and Fe concentrations equal to 6 and 11 wt% (cases ChFe6-800 and ChFe11-800), the composition of the gases was the same: 40% H<sub>2</sub>, 18% CO, 23% CH<sub>4</sub>, and 15% CO<sub>2</sub>. An increase in temperature to 900 °C with the same concentrations of Fe (cases ChFe6-900 and ChFe11-900) caused increases in the proportion of H<sub>2</sub> to 55–62% and CO to 24–38% and decreases of CH<sub>4</sub> to 4% and CO<sub>2</sub> to below 1%. Reducing the concentration of Fe to 1 wt% (case ChFe1-900) increased the share of CO<sub>2</sub> to 7%. Increasing the cracking temperature to 1000 °C (cases ChFe6-1000 and ChFe11-1000) caused the gas to consist of equal amounts of H<sub>2</sub> and CO with traces of other gases. A lack of catalyst (case Ch0Fe0-1000) caused the gas to consist of 42% H<sub>2</sub>, 31% CO, 11.5% CH<sub>4</sub>, and 12.7% CO<sub>2</sub>.



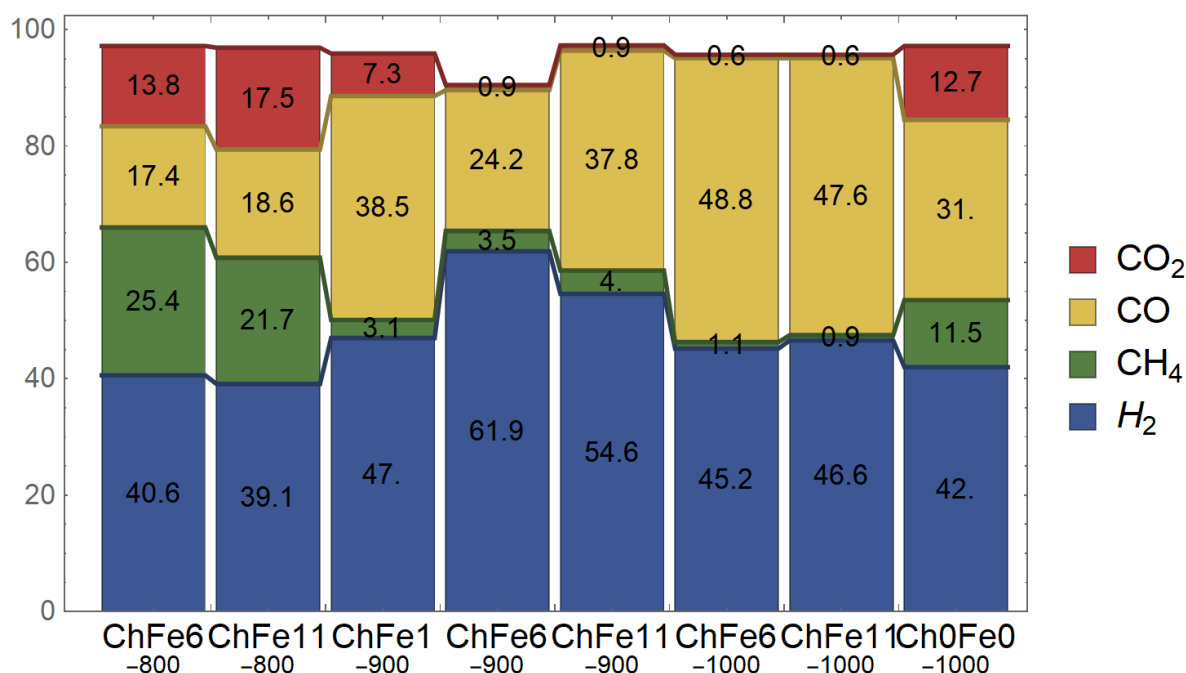


Figure 3. Gas composition (vol%) after RDF pyrolysis for different cases.

To heat the gas mixture to the temperature of 900 °C, about 2 MJ/kg is needed, which is about 10% of the waste heat of combustion. Such a relatively small amount of energy makes high-temperature cracking energy-efficient.

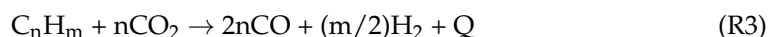
A comparison of the CO<sub>2</sub> and CO can be made from Figure 3. The increase in CO content is at the expense of CO<sub>2</sub>. Between cracking at 800 and 900 °C, the average CO<sub>2</sub> content decreased by 12% while the CO content increased by 15%, which can be explained by the Boudourd reaction. However, the further increase in CO content at 1000 °C cannot be explained in that way, because the CO<sub>2</sub> content is small and the CO increase is significant: a further 15 vol%. It seems that this may be caused by the cracking of tar occurring on the catalyst. When using a catalyst containing a high percentage of Fe, the high temperature promotes an increase in CO.

Between H<sub>2</sub> and CH<sub>4</sub>, there is no monotonic tendency that could be explained by a simple chemical mechanism. The increase in hydrogen content between 800 and 900 °C happens at the expense of CH<sub>4</sub>, but at a higher temperature, there is a decrease in the hydrogen content of the gas products. The lack of a char and iron catalyst (Ch0Fe0-1000), despite the high temperature of 1000 °C, results in a high content of CH<sub>4</sub>.

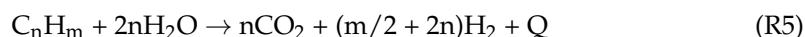
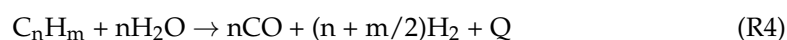
Gasification can be described by the following reactions [26]:



Dry reforming:



Steam reforming:



Methanation:





Oxidation reaction:



Water-char reaction: carbon from char may react with water:



Water gas shifting (WGS):



The reaction of pyrolysis and gas reduction in the presence of char (at 900 °C) with an Fe concentration of 6% or more results in gas with a concentration of 60% H<sub>2</sub>, 35% CO, and about 4% CH<sub>4</sub> with small amounts of higher-order hydrocarbons. This composition of the gas suggests that the dominant reactions during the pyrolysis and reduction reactions are methanation (R6), the water-char reaction (R12), and the oxidation reaction (R9) and (R11). In addition, due to the presence of water in RDF (max. 7%), the reactions R12, R6, and R7 can take place.

In the ChFe6-1000 and Ch0Fe0-1000 measurement series, measurements of the gaseous products were carried out. The use of a catalyst resulted in a significantly higher amount of gases (22 dm<sup>3</sup>) than in experiment Ch0Fe0-1000 without a catalyst (8 dm<sup>3</sup>). The ratio of gaseous products in the reservoir with and without a catalyst was 2.75.

Returning to the gas composition, the results shown in Figure 3 indicate a dependence on the process temperature but also on the concentration of Fe. While it is difficult to notice the differences between ChFe6 and ChFe11, the use of a low-iron catalyst ChFe1 is associated with a higher content of CO<sub>2</sub>. An even more pronounced effect can be seen in the absence of a char catalyst (Ch0Fe0, temperature 1000 °C), where despite very high temperatures, high levels of CO<sub>2</sub> and CH<sub>4</sub> remained. The impact of the catalyst and tar cracking process on the composition and calorific value of the RDF pyrolysis gas product is undoubtedly significant. In the pyrolysis process, the share of gaseous and liquid products changes. At temperatures above 500 °C, the char share is essentially constant, but depending on the content of the mineral parts, it can be different. The tar cracking will be conveniently determined not by the proportion of gases or liquids in the products but by the ratio of the mass of the gases to the mass of the liquids. As part of this research, a mass measurement of the gaseous and solid products was performed for the ChFe6-1000 series. The RDF mass loaded into the reactor was 32.1 g. The mass of char remaining in the reactor after pyrolysis was 12.9 g and the mass of the gases (H<sub>2</sub>, CO, and CH<sub>4</sub> only) measured was 16.6 g. Solid residues of 35 mg were measured in the scrubbers. The rest of the products were liquids (2.6 g), which were determined from the mass balance. The mass share of the noncondensing gases was 51.7%, that of the char products was 40.2%, and that of the liquid products was 8.1%. Therefore, the estimated ratio of gaseous to liquid products was 6.4. In fact, the amount of gas is underestimated and the gas-to-liquid ratio is greater because of the solubility of CO and H<sub>2</sub> in the water in the measuring tank. Furthermore, part of the liquid fraction may have remained in the cool silicate insulation and would be transformed into gases if allowed to flow through the catalyst.

The result of the ratio of gaseous to liquid products obtained in the experiment was compared with the results of other authors (Figure 4), which were divided into two groups. The first group consisted of the experiments by Efika et al. [17], Kardaś et al. [14], Ates et al. [18], Czajczyńska et al. [27], and Fekhar et al. [19], which were concerned only with MSW pyrolysis and are marked with dots. The second category of research concerned



both MSW pyrolysis and tar cracking and included Lu et al. [16], Al-Rahbi et al. [15], and Fekhar et al. [19], marked with squares, as well as the results of the present authors, which are marked with a diamond. Trend lines of the pyrolysis and cracked pyrolysis are plotted from the experimental points. The difference between the ratio of gaseous and liquid products is visible. The use of a catalyst and cracking results in a clear decomposition of tar into gaseous products. The current experiment decomposes the liquid to the gaseous phase to a high degree. In the case of pure MSW pyrolysis, the average mass of gaseous products does not exceed 200% of the mass of the liquid products. Basically, the use of ordinary MSW char as a catalyst greatly improves the efficiency of the liquid cracking, and at 900 °C, the mass ratio of gas to liquids exceeds 4, whereas at 1000 °C, it exceeds 6.

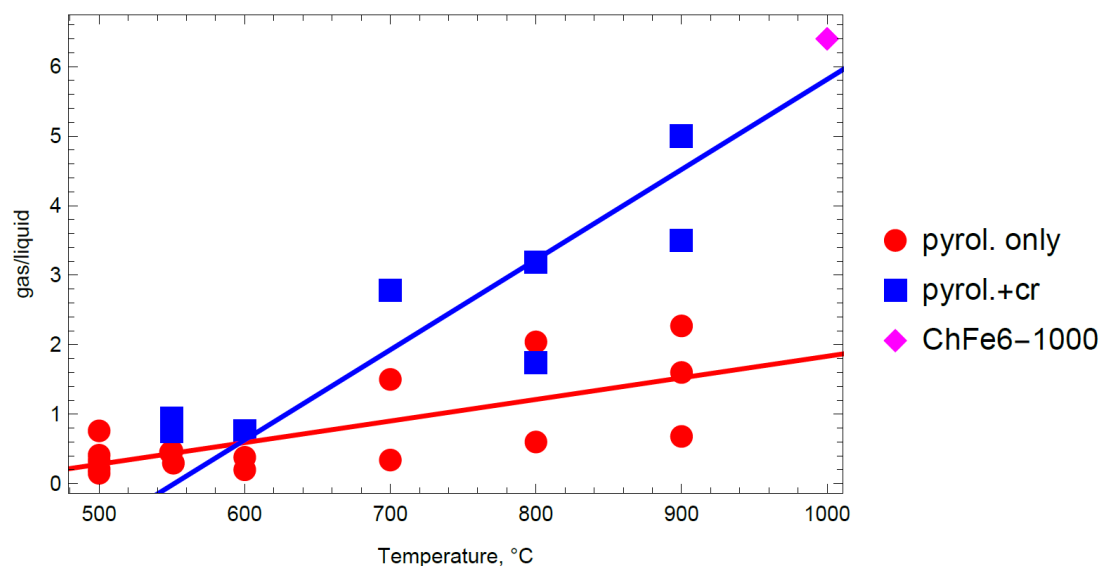


**Figure 4.** The ratio of the mass of gaseous products to the mass of liquid products as a function of temperature for pyrolysis and pyrolysis with tar cracking.

The pyrolysis process occurs primarily in the temperature range from 300 to 480 °C and lasts about 90 min. This means that the average stream of pyrolytic gases flows through the catalytic bed at an average of  $m_{pyr} = 0.21$  g/min. The density of pyrolytic gases  $\rho$  depends on the composition, temperature  $T$ , and pressure  $p$ . Taking the ideal gas state equation as a basis, the mixture density can be expressed by Equation (1):

$$\rho = \frac{P}{RT} \sum_i X_i M_i \quad (1)$$

where  $X_i$  is the molar fraction of component  $i$  in the mixture and  $M_i$  is its molar mass. The calculations assume that the tars are represented by toluene and their mass fraction is described by the blue line in Figure 4. The composition of the remaining products, that is,  $H_2$ ,  $CO$ ,  $CO_2$ ,  $CH_4$ ,  $N_2$ , and  $O_2$ , came from the measurements in Figure 3. The densities of the mixture  $\rho$  are presented in Table 4, from which it can be seen that the range of variation is between 0.15 and 0.27 kg/m<sup>3</sup>. The inner diameter of the pipe is 28 mm, which means that the cross-sectional area is  $A = 6.16 \times 10^{-4}$  m<sup>2</sup>, and the porosity  $\varepsilon$  of the bed inside the pipe is 0.56. The average gas flow velocity  $v$  is determined from the mass balance equation:

$$v = \frac{m_{pyr}}{A\varepsilon\rho} \quad (2)$$

The length of the bed is  $l = 0.2$  m and the residence time  $\Delta t$  in this zone is expressed by Equation (3):

$$\Delta t = \frac{l}{v} \quad (3)$$

The results of calculations of the gas flow velocity  $v$  and the gases' residence time  $\Delta t$  in the char bed are presented in Table 5. The residence time of the gases in the cracking catalytic zone is below 5.1 s. This is the time at which the catalytic tar decomposition occurs. This is a very short time compared to the gas residence time of tens of minutes in the experiments of Song et al. [20]. In the case of the Ch0Fe0-1000 experiment, the residence time is only slightly longer and amounts to 6.7 s.

**Table 5.** Gas density, velocity, and residence time in experiment series.

	$\rho$	$v$	$\Delta t$
Experiment	kg/m <sup>3</sup>	m/s	s
ChFe6-800	0.25	0.041	4.9
ChFe11-800	0.27	0.038	5.1
ChFe1-900	0.20	0.049	4.0
ChFe6-900	0.15	0.068	2.9
ChFe11-900	0.17	0.060	3.3
ChFe6-1000	0.18	0.058	3.4
ChFe11-1000	0.17	0.059	3.4
Ch0Fe0-1000	0.19	0.029	6.7

#### 4. Conclusions

The present paper has presented the results of research on RDF pyrolysis combined with catalytic tar cracking at high temperatures. The conducted experiments showed that RDF pyrolysis combined with the flow of the syngas through a source heated to a temperature of over 800 °C led to a significant change in the composition of the gases. In all these cases, the CO and H<sub>2</sub> contents increased, while the CO<sub>2</sub> and CH<sub>4</sub> contents decreased. The share of hydrogen in the gases was highest at a temperature of 900 °C. The gases' residence time in the catalytic zone was about 3–5 s.

**Author Contributions:** B.K.: Conceptualization, Investigation, Methodology; D.K.: Writing—original Draft, Conceptualization, Validation; Ł.H.: Investigation, Methodology; B.T.: Writing—Review and Editing. All authors have read and agreed to the published version of the manuscript.

**Funding:** This research received no external funding.

**Institutional Review Board Statement:** Not applicable.

**Informed Consent Statement:** Not applicable.

**Data Availability Statement:** Not applicable.

**Conflicts of Interest:** The authors declare no conflict of interest.

#### References

1. Eurostat. Municipal Waste Statistics. 2020. Available online: [https://ec.europa.eu/eurostat/statistics-explained/index.php/Municipal\\_waste\\_statistics](https://ec.europa.eu/eurostat/statistics-explained/index.php/Municipal_waste_statistics) (accessed on 12 December 2021).
2. Klimczak, B. The largest waste incineration plant in Pomerania. *Biomasa* **2020**, *6*, 44–46.
3. Cyranka, M.; Jurczyk, M. Experimental tests of co-combustion of pelletized leather tannery wastes and hardwood pellets. *Agric. Eng.* **2016**, *20*, 23–33.
4. Working Group. *Waste to Energy State of the Art Report*; International Solid Waste Association, 2012. Available online: [https://www.nswai.org/docs/ISWA6\\_7-000-2\\_WtE\\_State\\_of\\_the\\_Art\\_Report\\_2012\\_Revised\\_November\\_2013.pdf](https://www.nswai.org/docs/ISWA6_7-000-2_WtE_State_of_the_Art_Report_2012_Revised_November_2013.pdf). (accessed on 12 December 2021).
5. Gondal, I.A.; Masood, S.A.; Khan, R. Green hydrogen production potential for developing a hydrogen economy in Pakistan. *Int. J. Hydrogen Energy* **2018**, *43*, 6011–6039. [CrossRef]
6. Uddin, M.N.; Wan Daud, W.M.A.; Abbas, H.F. Potential hydrogen and non-condensable gases production from biomass pyrolysis: Insights into the process variables. *Sustain. Energy Rev.* **2013**, *27*, 204–224. [CrossRef]
7. Al-Rahbi, A.S.; Williams, P.T. Hydrogen-rich syngas production and tar removal from biomass gasification using sacrificial tyre pyrolysis char. *Appl. Energy* **2017**, *190*, 501–509. [CrossRef]

8. Yamada, S.; Shimizu, M.; Miyoshi, F. Thermoselect Waste Gasification and Reforming Process. JFE Technical Report No. 3 (July 2004). Available online: <https://www.jfe-steel.co.jp/en/research/report/003/pdf/003-05.pdf>. (accessed on 12 December 2021).
9. Kardaś, D.; Kluska, J.; Kazimierski, P.; Heda, Ł. *Container installation for gasification of municipal waste in Nowy Dwór*; Nowa Energia: Racibórz, Poland, 2017; D. Kubek i M. Marchwiak Spółka Cywilna.
10. Arena, U. Process and technological aspects of municipal solid waste gasification. A review. *Waste Manag.* **2012**, *32*, 625–639. [[CrossRef](#)]
11. Campuzano, F.; Brown, R.C.; Martínez, J.D. Auger reactors for pyrolysis of biomass and wastes. *Renew. Sustain. Energy Rev.* **2019**, *102*, 372–409. [[CrossRef](#)]
12. Panepinto, D.; Zanetti, M. Municipal solid waste incineration plant: A multi-step approach to the evaluation of an energy-recovery configuration. *Waste Manag.* **2018**, *73*, 332–341. [[CrossRef](#)]
13. Devi, L.; Ptasinski, K.J.; Janssen, F.J. A review of the primary measures for tar elimination in biomass gasification processes. *Biomass Bioenergy* **2003**, *24*, 125–140. [[CrossRef](#)]
14. Kardaś, D.; Kluska, J.; Klein, M.; Kazimierski, P.; Heda, Ł. *Theoretical and Experimental Aspects of Wood and Waste Pyrolysis*; Wydawnictwo UWM: Olsztyn, Poland, 2014.
15. Al-Rahbi, A.S.; Onwudili, J.A.; Williams, P.T. Thermal decomposition and gasification of biomass pyrolysis gases using a hot bed of waste derived pyrolysis char. *Bioresour. Technol.* **2016**, *204*, 7179. [[CrossRef](#)] [[PubMed](#)]
16. Lu, P.; Huang, Q.; Chi, Y.; Wang, F.; Yan, J. Catalytic cracking of tar derived from the pyrolysis of municipal solid waste fractions over biochar. *Proc. Combust. Inst.* **2019**, *37*, 26732680. [[CrossRef](#)]
17. Efika, E.C.; Onwudili, J.; Williams, P.T. Products from the high temperature pyrolysis of RDF at slow and rapid heating rates. *J. Anal. Appl. Pyrolysis* **2015**, *112*, 14–22. [[CrossRef](#)]
18. Ates, F.; Miskolczi, N.; Borsodi, N. Comparison of real waste (MSW and MPW) pyrolysis in batch reactor over different catalysts. Part I: Product yields, gas and pyrolysis oil properties. *Bioresour. Technol.* **2013**, *133*, 443–454. [[CrossRef](#)] [[PubMed](#)]
19. Fekhar, B.; Zsinka, V.; Miskolczi, N. Thermo-catalytic co-pyrolysis of waste plastic and paper in batch and tubular reactors for in-situ product improvement. *J. Environ. Manag.* **2020**, *269*, 110741. [[CrossRef](#)] [[PubMed](#)]
20. Song, Q.; Zhao, H.; Jia, J.; Yang, L.; Lv, W.; Bao, J.; Shu, X.; Gu, Q.; Zhang, P. Pyrolysis of municipal solid waste with iron-based additives: A study on the kinetic, product distribution and catalytic mechanisms. *J. Clean. Prod.* **2020**, *258*, 120682. [[CrossRef](#)]
21. Shen, Y.; Zhao, P.; Shao, Q.; Takahashi, F.; Yoshikawa, K. In situ catalytic conversion of tar using rice husk char/ash supported nickel-iron catalysts for biomass pyrolytic gasification combined with the mixing-simulation in fluidized-bed gasifier. *Appl. Energy* **2015**, *160*, 808–819. [[CrossRef](#)]
22. Zhao, H.; Li, Y.; Song, Q.; Liu, S.; Ma, Q.; Ma, L.; Shu, X. Catalytic reforming of volatiles from co-pyrolysis of lignite blended with corn straw over three different structures of iron ores. *J. Anal. Appl. Pyrolysis* **2019**, *144*, 104714. [[CrossRef](#)]
23. Al-Salem, S.; Antelava, A.; Constantinou, A.; Manos, G.; Dutta, A. A review on thermal and catalytic pyrolysis of plastic solid waste (PSW). *J. Environ. Manag.* **2017**, *197*, 177–198. [[CrossRef](#)]
24. Al-Asadi, M.; Miskolczi, N. High Temperature Pyrolysis of Municipal Plastic Waste Using Me/Ni/ZSM-5 Catalysts: The Effect of Metal/Nickel Ratio. *Energies* **2020**, *13*, 1284. [[CrossRef](#)]
25. Veses, A.; Sanahuja-Parejo, O.; Soledad Calln, M.; Murillo, R.; Garca, T. A combined two-stage process of pyrolysis and catalytic cracking of municipal solid waste for the production of syngas and solid refuse de-rived fuels. *Waste Manag.* **2020**, *101*, 171–179. [[CrossRef](#)] [[PubMed](#)]
26. Shen, Y. Chars as carbonaceous adsorbents/catalysts for tar elimination during biomass pyrolysis or gasification. *Renew. Sustain. Energy Rev.* **2015**, *43*, 281–295. [[CrossRef](#)]
27. Czajczyńska, D.; Anguilano, L.; Ghazal, H.; Krzyżyńska, R.; Reynolds, A.J.; Spencer, N.; Jouhara, H. Potential of pyrolysis processes in the waste management sector. *Therm. Sci. Eng. Prog.* **2017**, *3*, 171–197. [[CrossRef](#)]

